doi:10.1246/cl.2012.674

Published on the web June 16, 2012

Effects of Alkoxy Substitution on the Optical Properties of 9,10-Anthraquinone and Anthracene: 2,3,6,7-Tetrapropoxy-substituted vs. 2,6-Dipropoxy-substituted Derivatives

Akira Ohta,*[1] Kazuki Hattori,[1] Yui Kusumoto,[2] Takeshi Kawase,[2]
Takashi Kobayashi,[3] Hiroyoshi Naito,[3] and Chitoshi Kitamura*[2]
[1]*Department of Chemistry, Faculty of Science, Shinshu University, 3-1-1 Asahi, Matsumoto, Nagano 390-8621*
[2]*Department of Materials Science and Chemistry, Graduate School of Engineering, University of Hyogo, 2167 Shosha, Himeji, Hyogo 671-2280*
[3]*Department of Physics and Electronics, Graduate School of Engineering, Osaka Prefecture University, 1-1 Gakuen-cho, Naka-ku, Sakai, Osaka 599-8531*

(Received April 6, 2012; CL-120303; E-mail: aohta@shinshu-u.ac.jp, kitamura@eng.u-hyogo.ac.jp)

2,3,6,7-Tetrapropoxy- and 2,6-dipropoxy-substituted 9,10-anthraquinone (**AQ**) and anthracene (**ANT**) derivatives were synthesized, and their optical properties in solution and in the solid state were investigated. In **AQ**s, the tetrapropoxy derivative exhibited a red shift of absorption in comparison with the dipropoxy derivative and **ANT**. In contrast, in **ANT**s, the dipropoxy derivative exhibited a red shift of absorption and fluorescence in comparison with the tetrapropoxy derivative and **ANT**. The electronic effects of alkoxy substitution could be explained by TD-DFT calculations.

9,10-Anthraquinone (**AQ**) and anthracene (**ANT**) are principle, important molecules because of their industrial and academic importance (Chart 1). A large number of **AQ** derivatives have been manufactured as dyes and pigments. **ANT** derivatives have also received considerable attention owing to their blue emission[1] and photoconductivity.[2] Thus, both **AQ** and **ANT** derivatives are basic and versatile molecules as colorants and optoelectronic materials.

Since the control of the fluorescence properties of **ANT** in the solid state was first reported by Tohnai's group,[3] who used organic salts of anthracene-2,6-disulfonic acid with alkyl amines, it has become important to understand the dependence of the solid-state optical properties on molecular arrangements and the factors that determine the nature of molecular packing.[4] Recently, we studied the solid-state optical properties of 1,4,5,8-tetraalkylanthracenes,[5] demonstrating that alkyl substitution on the anthracene ring is effective in tuning the fluorescent properties in the solid state. Given the results of our studies on the effects of substitution on the optical properties of **AQ** and **ANT**, we have been interested in the effects of the alkoxy substitution instead of alkyl groups. Substitution by electron-donating alkoxy groups is expected to extend π systems and result in a bathochromic shift of the peaks. Also, the introduction of alkoxy substituents can easily be performed by the Williamson reaction because of the higher availability of hydroxy-substituted **AQ**s. However, to the best of our knowledge, research and comparison of the optical properties of 2,3,6,7-tetraalkoxy- and 2,6-dialkoxy-substituted **AQ**s and **ANT**s have not been conducted. The modulation of the electronic structures of **AQ**s and **ANT**s requires an understanding of structure–property relationships regarding substituent effects. Moreover, the alkoxy chain length may affect the solid-state optical properties. Here we report the results of our investigations focusing on the effects of the alkoxy substitution on the optical properties in solution and in the solid state of tetrapropoxy- and dipropoxy-substituted **AQ** and **ANT** derivatives **1a**, **1b**, **2a**, and **2b**. The propoxy group was chosen for the preliminary screening in expectation of moderate solubility in organic solvents and crystallization in the solid state.

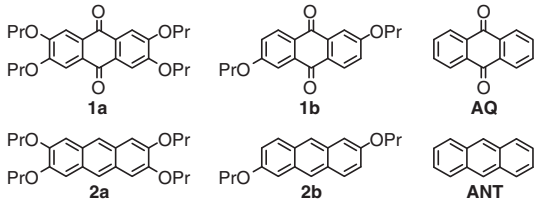

Chart 1.

The preparation of **1a**, **1b**, **2a**, and **2b** is shown in Schemes S1 and S2.[6] When we obtained these propoxy-substituted molecules, we noticed differences in color between **1a** and **1b** and between **2a** and **2b**. **1a** is slightly yellower and lighter than **1b**; while **2b** is faintly yellow but **2a** is colorless. The photophysical properties of **1a**, **1b**, **2a**, and **2b**, together with **AQ** and **ANT**, were investigated (Figures 1 and 2, and Table 1). The patterns of UV–vis absorption spectra in solution and the Kubelka–Munk spectra in the solid state differ significantly among **AQ**s and among **ANT**s (Figure 1). In the solution spectra of **1a** and **1b** (Figure 1a), the peaks assigned to the allowed π–π^* transition are observed at 344 and 348 nm, respectively; both are red-shifted in comparison with **AQ** (325 nm). In addition, relatively weak bands, which can be characterized as the forbidden n–π^* transitions, appear at approximately 370–500 nm (a broad peak at 402 nm) for **1a** and 370–440 nm (a shoulder at approximately 380 nm) for **1b**. In the solid state (Figure 1c), the bands based on the forbidden transitions in solution become large, resulting in an obvious red shift of tetrapropoxy-substituted **1a** (optical absorption edge (λ_{edge}) is 501 nm), while the λ_{edge} of dipropoxy-substituted **1b** (453 nm) is in close agreement with that of nonsubstituted **AQ** (460 nm). On the other hand, interestingly enough, the spectral profiles of **ANT**s display completely different substitution effects (Figures 1b and 1d). Thus, the longest absorption maximum (λ_{max}) in solution of tetrapropoxy-substituted **2a** (373 nm), which is assigned to the allowed π–π^* transition, is rather blue-shifted in comparison to that of nonsubstituted **ANT** (378 nm), although dipropoxy-substituted **2b** (404 nm) shows a

relatively large red shift from **ANT**. The solid-state absorption spectra also display similar behavior. Both λ_{max} and λ_{edge} values in KBr pellets are in the following order: **2b** (412 and 450 nm) > **ANT** (405 and 425 nm) > **2a** (375 and 411 nm). With regard to the fluorescence properties, all **AQ**s were nonemissive, and their fluorescent quantum yields (Φ_F) were nearly zero in solution and in the solid state. In contrast, the Φ_F values of **ANT**s differed depending upon the substitution pattern of the alkoxy groups (Table 1). The Φ_F of **2a** in CH_2Cl_2 is 0.22,

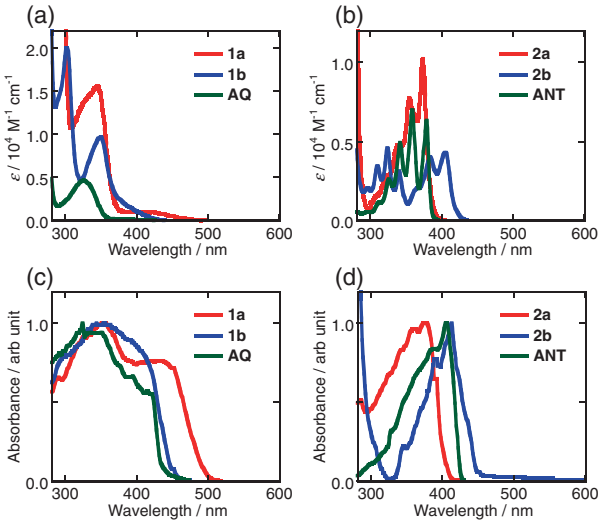

Figure 1. UV–vis absorption spectra in CH_2Cl_2 of (a) **1a**, **1b**, and **AQ**, and (b) **2a**, **2b**, and **ANT**, and the Kubelka–Munk spectra in KBr pellets of (c) **1a**, **1b**, and **AQ**, and (d) **2a**, **2b**, and **ANT**.

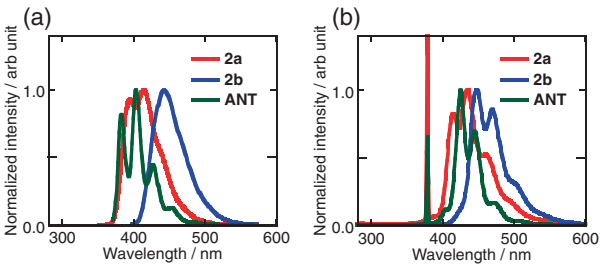

Figure 2. Fluorescence spectra of **2a**, **2b**, and **ANT** (a) in CH_2Cl_2 and (b) in the crystalline powder form.

a value considerably smaller than that of **2b** ($\Phi_F = 0.63$). Then, it is slightly smaller than that of **ANT** ($\Phi_F = 0.32$).[7] The Φ_F values in the solid state ($\Phi_F = 0.12$ for **2a** and $\Phi_F = 0.56$ for **2b**) are slightly smaller in comparison with those in solution. The fluorescence spectrum of **2a** in solution displays a vibronic structure. Here the emission maxima (λ_{em}) are 393 and 414 nm and are slightly red-shifted in comparison with **ANT** (382 and 403 nm). The fluorescence spectrum of **2b** shows one broad band ($\lambda_{em} = 442$ nm), which is more red-shifted than the other **ANT**s. In short, in the **AQ** system, tetrapropoxy substitution results in a red shift of absorption; on the other hand, in the **ANT** system, tetrapropoxy substitution results in the blue shifts of absorption and fluorescence.

To investigate the apparently irrational effects of the alkoxy substitution on the optical properties of **AQ**s and **ANT**s, we carried out time-dependent density functional theory (TD-DFT) calculations at the B3LYP/6-31G(d) level using methoxy-substituted **AQ**s, **1c** and **1d**, and **ANT**s, **2c** and **2d**, as model compounds.[9] We assumed that the molecules are coplanar and that the symmetry groups of the tetramethoxy and dimethoxy derivatives are D_{2h} (**1c** and **2c**) and C_{2h} (**1d** and **2d**), respectively (Figure 3). Both **1c** and **1d** has the first to third lowest forbidden transition bands and the fourth lowest allowed π–π^* transition band (Figures S1 and S2, and Table S1).[6] The lowest energy transition in **1c** is primarily a HOMO to LUMO forbidden transition (2.68 eV, 462 nm), although those in **1d** are HOMO–2 to LUMO (70%) and HOMO–3 to LUMO+1 (11%) forbidden transitions (3.01 eV, 412 nm). In contrast, the lowest energy transition in **ANT**s is a HOMO to LUMO π–π^* transition (Figure 4 and Table S2). The breakdown of D_{2h} or C_{2h} symmetry by molecular vibrations and C–O rotations in alkoxy

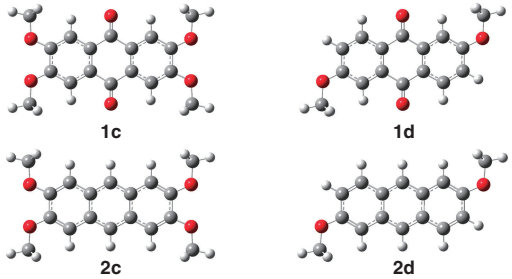

Figure 3. Optimized structures of tetramethoxy and dimethoxy derivatives.

Table 1. Absorption and fluorescence spectroscopic data of **1a**, **1b**, **AQ**, **2a**, **2b**, and **ANT**

Compound	In CH_2Cl_2			In the solid state			
	Absorption	Fluorescence[a]		Absorption[c]		Fluorescence[d,e]	
	λ_{max}/nm (log ε)	λ_{em}/nm	Φ_F[b]	λ_{max}/nm	λ_{edge}/nm	λ_{em}/nm	Φ_F[f]
1a	344 (4.19), 402 (3.02)	—	<0.01	440	501	—	<0.01
1b	348 (3.99), 380 sh (3.32)	—	<0.01	415 sh	453	—	<0.01
AQ	325 (3.67), 370 (2.27)	—	<0.01	407	460	—	<0.01
2a	354 (3.89), 373 (4.01)	393, 414	0.22	375	411	415, 433	0.12
2b	383 (3.60), 404 (3.63)	442	0.63	412	450	435, 464	0.56
ANT	358 (3.85), 378 (3.80)	382, 403	0.32[g]	405	425	424, 444	0.64[h]

[a]Excited at 355 nm for **1b**, **2b**, and **AQ**, and at 335 nm for the other compounds. [b]Fluorescence quantum yields were determined using 9,10-diphenylanthracene as the standard. [c]In KBr pellets. [d]In the crystalline powder form. [e]Excited at 377 nm. [f]Absolute quantum yields, which were measured with an integrating sphere. [g]Reference 7. [h]Reference 8.

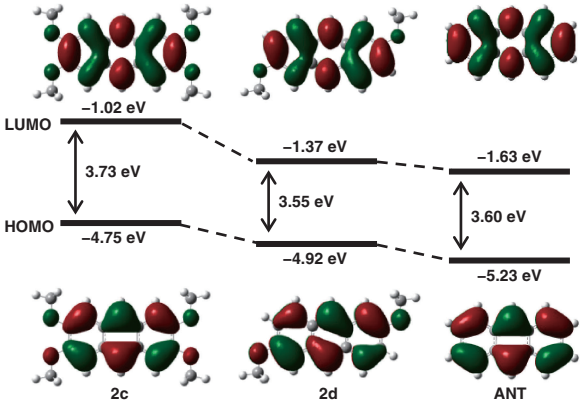

Figure 4. HOMO and LUMO energy levels of **2c**, **2d**, and **ANT**.

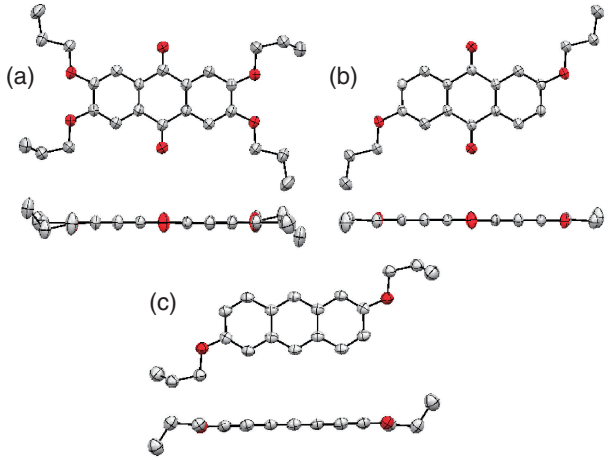

Figure 5. ORTEP drawings of (a) **1a**, (b) **1b**, and (c) **2b**.

substituents would facilitate the forbidden optical transitions. The red shift of **1a** compared with **1b** in the absorption spectra can be ascribed to the difference in the lowest transition energy of the forbidden transition in **AQ**s. The introduction of electron-donating methoxy groups on **ANT** increases both the HOMO and LUMO energies (Figure 4). The HOMO and LUMO energies of **2d** were calculated to be −4.92 and −1.37 eV, and those of **2c** were −4.75 and −1.02 eV, respectively. Interestingly, the HOMO–LUMO gap of **2c** (3.73 eV) is larger than that of **2d** (3.55 eV), and the latter is smaller than the HOMO–LUMO gap of **ANT** (3.60 eV). Thus, the estimated HOMO–LUMO gaps are in the following order: **2c** > **ANT** > **2d**. This result agrees well with the experimental order of the longest wavelengths of the absorption peak (λ_{max}) in solution, as can be seen in Table 1 and Figure 1b. As a result, the 2,3,6,7-tetramethoxy substitution on **ANT** increases the LUMO energy slightly more than the corresponding HOMO energy. However, the 2,6-dimethoxy substitution on **ANT** increases the HOMO energy slightly more than the corresponding LUMO energy. In addition, there is a difference in oscillator strength between **2c** and **2d** (Table S2).[6] The oscillator strength in the HOMO to LUMO π–π^* transition in **2c** ($f = 0.021$) is lesser than that in **2d** ($f = 0.050$). This would be a cause of lower fluorescence quantum yields of tetrapropoxy-substituted **2a** in comparison with dipropoxy-substituted **2b**. TD-DFT calculations revealed that the alkoxy substitution at the 2,6- or 2,3,6,7-positions remarkably affects the energies and the oscillator strength in the lowest energy transition; these differences would bring about the differences in the optical properties.

Because we succeeded in obtaining single crystals of **1a**, **1b**, and **2b**, X-ray analysis was performed to investigate conformations of alkoxy substituents,[6,10] which may affect the solid-state optical properties. All molecules possess a center of symmetry and, hence, are characterized by C_i symmetry. The alkoxy conformations vary among the molecules (Figure 5). Molecule **1b** has a planar structure in which propoxy groups assume a trans-planar (*zigzag*) conformation. In contrast, molecule **2b** has a different conformation from **1b**. The O–C–C–C moiety of the propoxy group in **2b** gives rise to a *gauche* conformation with a torsion angle of 63.43°. On the other hand, molecule **1a** displays a more complicated structure, involving one pair of *zigzag* propoxy groups at the 3,7-positions and another pair of *gauche* propoxy groups (torsion angle, 66.20°) at the 2,6-positions. The results of TD-DFT calculations of **1a**, **1b**, and **2b** using the geometry obtained by X-ray analysis were almost identical with those of **1c**, **1d**, and **2d**, respectively (Figures S4–S6, and Table S3).[6] Investigation of the effects of the alkoxy chain length on the solid-state optical properties is currently in progress.

In conclusion, we analyzed the optical properties of 2,3,6,7-tetrapropoxy and 2,6-dipropoxy **AQ** and **ANT** derivatives. The optical properties in solution and in the solid state demonstrated that, in **AQ**s, tetrapropoxy-substituted **1a** exhibits a red shift of absorption in comparison with nonsubstituted **AQ** and dipropoxy-substituted **1b**. In contrast, in **ANT**s, the tetrapropoxy-substituted **2a** displays a red shift of absorption and fluorescence in comparison with nonsubstituted **ANT** and dipropoxy-substituted **2b**. We succeeded in explaining the apparently irrational behavior of the optical properties relative to the alkoxy substitution by TD-DFT calculations.

This work was partly supported by a Grant-in-Aid for Scientific Research (KAKENHI) (C) (No. 23550161) from JSPS and KAKENHI on Innovative Areas (No. 23108720, "pi-Space") from MEXT.

References and Notes

1 Z. Zhang, Y. Zhang, D. Yao, H. Bi, I. Javed, Y. Fan, H. Zhang, Y. Wang, *Cryst. Growth Des.* **2009**, *9*, 5069.
2 M. Pope, C. E. Swenberg, *Electronic Processes in Organic Crystals and Polymers*, Oxford University Press, New York, **1999**.
3 Y. Mizobe, N. Tohnai, M. Miyata, Y. Hasegawa, *Chem. Commun.* **2005**, 1839.
4 S. Varghese, S. Das, *J. Phys. Chem. Lett.* **2011**, *2*, 863.
5 C. Kitamura, Y. Abe, N. Kawatsuki, A. Yoneda, K. Asada, T. Kobayashi, H. Naito, *Mol. Cryst. Liq. Cryst.* **2007**, *474*, 119.
6 Supporting Information is available electronically on the CSJ-Journal Web site, http://www.csj.jp/journals/chem-lett/index.html.
7 M. Shimizu, K. Oda, T. Bando, T. Hiyama, *Chem. Lett.* **2006**, *35*, 1022.
8 R. Katoh, K. Suzuki, A. Furube, M. Kotani, K. Tokumaru, *J. Phys. Chem. C* **2009**, *113*, 2961.
9 TD-DFT calculations were performed at the B3LYP/6-31G(d) level using Gaussian 09 program. M. J. Frisch, et al., *Gaussian 09 (Revision A.02)*, Gaussian, Inc., Wallingford CT, **2009**.
10 Crystallographic data have been deposited at Cambridge Crystallographic Data Centre: CCDC-874655 for **1a**, CCDC-874656 for **1b**, and CCDC-874657 for **2b**. Copies of the data can be obtained free of charge via http://www.ccdc.cam.ac.uk/conts/retrieving.html.

